VIBRATION ISOLATION SYSTEM USING ZERO-POWER MAGNETIC SUSPENSION WITH A WEIGHT SUSPENSION MECHANISM

Takeshi MIZUNO, Daisuke KISHITA, Md. Emdadul HOQUE, Masaya TAKASAKI and Yuji ISHINO

Department of Mechanical Engineering, Saitama University
Shimo-Okubo 255, Saitama 338-8570, Japan
Phone: ++ 81 48 858 3455, Fax: ++81 48 856 2577
E-mail: mizar@mech.saitama-u.ac.jp

Abstract: Vibration isolation system using zero-power magnetic suspension is modified to be equipped with a weight support mechanism. The original system has a problem that the whole weight of the isolation table must be supported solely by the attractive force produced by permanent magnets. It is an obstacle to develop large isolation tables. In order to overcome this obstacle, a weight support mechanism is introduced in parallel with the serial connection of a zero-power magnetic suspension system and a normal spring. It can reduce the static load force that the zero-power magnetic suspension has to support. The basic characteristics of the modified system are shown analytically. Experimental study demonstrates that the modified system maintains infinite stiffness against direct disturbance even if such a weight support mechanism is added.

Keywords: magnetic suspension, magnetic bearings, active control, vibration, springs, accelerometers, mechanical systems, passive compensation, zero error.

1. INTRODUCTION

Demands for high-performance vibration isolation systems have been increasing in various scientific and industrial fields. There are two kinds of vibration to be reduced by vibration isolation system (Yasuda and Ikeda, 1993). One is vibration transmitted from ground through suspension (spring). The other is vibration caused by disturbances acting on the isolation table (direct disturbance). Lower stiffness of suspension is better for reducing the former while higher stiffness is better for suppressing the latter. A trade-off between them is inevitable in conventional passive-type vibration isolation systems so that their performances are limited.

The author has proposed a new approach to breaking through the trade-off (Mizuno, 2002). The proposed vibration isolation system is characterized by using zero-power magnetic suspension. Since a zero-power suspension system behaves as if it has a negative stiffness, infinite stiffness against disturbances on the isolation table can be achieved by combining it with a normal spring. It enables the system to have good characteristics both in reducing vibration transmitted from ground and in suppressing direct vibration.

However, the original system has several problems. One of them is that the whole weight of the isolation table is supported by zero-power magnetic suspension. Therefore when the isolation table is large, it is necessary to use a lot of permanent magnets. Another problem is that a ferromagnetic part of the isolation table must be under the middle table, because zero-power magnetic suspension can produce only attractive force. It makes the structure of vibration isolation system rather complex.

In order to overcome these problems, Mizuno (2003) has proposed to introduce an auxiliary suspension for supporting the weight of the isolation table in parallel with the serial connection of positive and negative springs. In this paper, the basic characteristics of the modified vibration isolation system are studied both theoretically and experimentally.

2. VIBRATION ISOLATION SYSTEM USING ZERO-POWER MAGNETIC SUSPENSION

2.1 Basic Idea

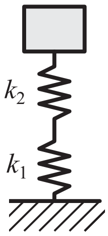

Fig.1 Series springs

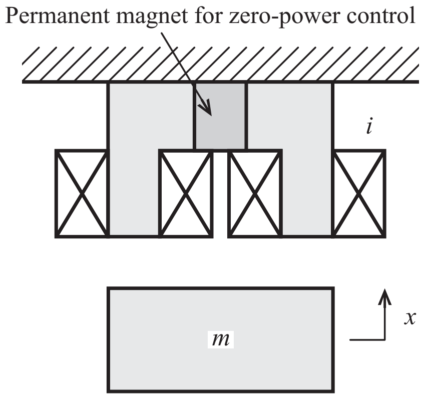

Fig.2 Basic model of zero-power magnetic suspension system

First it is shown that infinite stiffness can be realized by connecting a normal spring with a spring that has negative stiffness (Mizuno, 2002). When two springs with spring constants of k_1 and k_2 are connected in series as shown by Fig.1, the total stiffness k_c is given by

$$k_c = \frac{k_1 k_2}{k_1 + k_2} . \tag{1}$$

This equation shows that the total stiffness becomes lower than that of each spring when normal springs are connected. However, if one of the springs has negative stiffness that satisfies

$$k_1 = -k_2 , \tag{2}$$

the resultant stiffness becomes infinite, that is

$$|k_c| = \infty . \tag{3}$$

This research applies this principle of generating high stiffness against direct disturbance acting on vibration isolation systems.

2.2 Zero-power Magnetic Suspension

Systems containing passive elements with negative stiffness are generally unstable because they generate force in the direction opposite to restoring. Active control is, therefore, necessary to realize negative stiffness without instability. Zero-power control is used in this research.

Model. Figure 2 shows a single-degree-of-freedom-of-motion model for describing zero-power magnetic suspension (Mizuno and Takemori, 2002). The suspended object with mass of m is assumed to move only in the vertical direction translationally. The equation of motion is given by

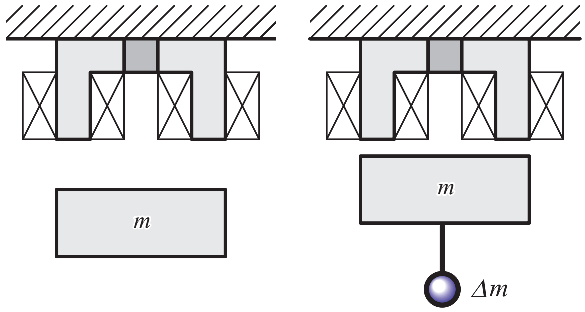

(a) Original equilibrium state (b) New equilibrium state

Fig.3 Basic characteristic of zero-power magnetic suspension system

$$m\ddot{x}(t) = k_s x(t) + k_i i(t) + f_d(t) , \tag{4}$$

where x : displacement of the suspended object, k_s : gap-force coefficient of the magnet, k_i : current-force coefficient of the magnet, i : control current, f_d : disturbance acting on the suspended object.

Controller. The zero-power control operates to accomplish

$$\lim_{t\to\infty} i(t) = 0 \quad \textit{for stepwise disturbances}. \tag{5}$$

The controller achieving the control objective (5) is generally represented by

$$I(s) = -\frac{s\tilde{h}(s)}{g(s)} X(s) , \tag{6}$$

where $g(s)$ and $\tilde{h}(s)$ are coprime polynomials in s and selected for the closed-loop system to be stable (Mizuno and Takemori, 2002).

Negative Stiffness. When a constant force F_0 is applied to the suspended object, the suspended object is maintained at the position satisfying

$$0 = k_s x(\infty) + k_i i(\infty) + F_0 , \tag{7}$$

in the steady states. In the zero-power control system, the coil current converges to zero, that is,

$$i(\infty) = 0 . \tag{8}$$

Therefore,

$$x(\infty) = -\frac{F_0}{k_s} . \tag{9}$$

The negative sign appearing in the right-hand side verifies that the new equilibrium position is in the direction opposite to the applied force. It indicates that the zero-power control system behaves as if it has negative stiffness. When an external force is applied to the mass in common mass-spring systems, the mass moves to the direction of the applied force.

In the zero-power controlled system, the suspended object moves in the opposite direction as shown in Fig.3.

2.3 System Configuration

Figure 4 shows the configuration of one of the proposed vibration isolation systems (Mizuno, 2002). A middle table is connected to the base through a spring k_1 and a damper c_1 that work as a conventional vibration isolator. An electromagnet for zero-power magnetic suspension is fixed to the middle table. The part of an isolation table facing the electromagnet (*reaction part*) is made of permanent magnets for zero-power suspension and soft iron material confining magnetic fields produced by the permanent magnets.

This system can reduce vibration transmitted from ground by setting k_1 small and at the same time have infinite stiffness against direct disturbance by setting the amplitude of negative stiffness equal to k_1.

2.4 Introduction of Weight Suspension Mechanism

In the system shown by Fig.4, the whole weight of the isolation table is supported by zero-power magnetic suspension. When the isolation table is large, therefore, a lot of permanent magnets are necessary for suspending the weight, which will raise the cost. Another problem expected in putting the proposed system to practical use is that the reaction part must be installed under the middle table as shown by Fig.4. It is because hybrid magnetic can produce only attractive force. It makes the structure of vibration isolation system rather complex.

These problems can be overcome by introducing an auxiliary suspension for supporting the weight. The concept is explained with Fig.5. A spring k_d is added in parallel with the serial connection of positive and negative springs. The total stiffness $\tilde{k}_c$ is given by

$$\tilde{k}_c = \frac{k_1 k_2}{k_1 + k_2} + k_d . \tag{10}$$

When Eq.(2) is satisfied, the resultant stiffness becomes infinite for any finite value of k_d.

$$\left|\tilde{k}_c\right| = \infty . \tag{11}$$

Figure 6 shows the configuration of one of the proposed vibration isolation systems. A spring k_d together with a damper c_d is inserted between the isolation table and the base. The spring is set to produce upward force in the equilibrium state. It reduces the static load force that the zero-power magnetic suspension has to support. Moreover, when

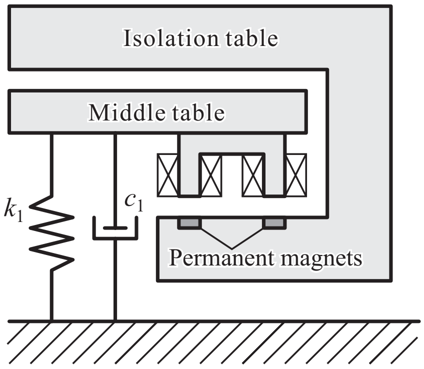

Fig.4 Original configuration of vibration isolation system using zero-power magnetic suspension

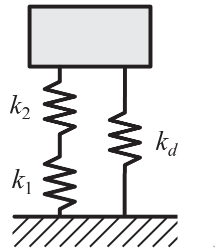

Fig.5 Introduction of a parallel spring

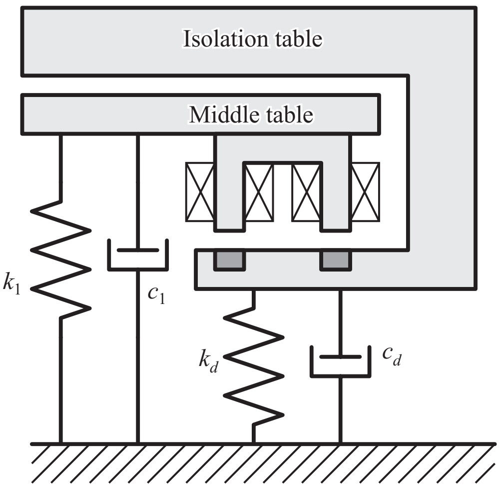

Fig.6 Configuration of vibration isolation system with a weight support mechanism

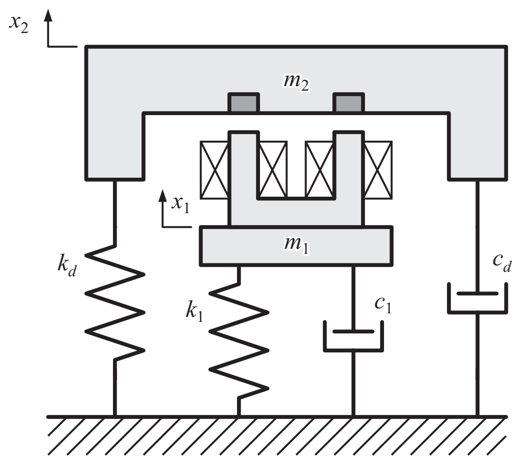

Fig.7 Another configuration of vibration isolation system with a weight support mechanism

the upward force is greater than the gravitational force, the zero-power magnetic suspension must produce downward force so that the configuration is modified as shown by Fig.7. Since the reaction part is installed above the middle table, the structure is simpler than the original shown by Fig.4. It is to be noted that the performance of isolation from ground vibration can be maintained by using a soft spring as k_d.

3. ANALYSIS

3.1 Basic Equations

The model shown by Fig.7 is treated in this work. The equations of motion about the translation motion in the vertical direction are

$$m_1\ddot{x}_1 = -m_1 g + k_1 \Delta x_1 - k_1(x_1 - x_0) - c_1(\dot{x}_1 - \dot{x}_0) + f_e, \tag{12}$$

$$m_2\ddot{x}_2 = -m_2 g + k_d \Delta x_2 - k_d(x_2 - x_0) - c_d(\dot{x}_2 - \dot{x}_0) - f_e + f_d, \tag{13}$$

where x_0, x_1, x_2: displacements of the floor, the middle mass and the isolation table, f_e: attractive force of the hybrid magnet, f_d: direct disturbance acting on the isolation table, Δx_1: initial compressed length of spring k_1, Δx_3: initial compressed length of spring k_d.

The attractive force of the hybrid magnet is approximately represented by

$$f_e = \bar{f}_e + k_s(x_1 - x_2) + k_i i, \tag{14}$$

where $\bar{f}_e$: attractive force in the equilibrium states. The following are satisfied in the equilibrium states.

$$k_1 \Delta x_1 - m_1 g + \bar{f}_e = 0, \tag{15}$$

$$k_d \Delta x_2 - m_2 g - \bar{f}_e = 0. \tag{16}$$

From Eq.(16), we get

$$\bar{f}_e = k_d \Delta x_2 - m_2 g. \tag{17}$$

Therefore, the condition that allows the configuration shown by Fig.7 is given by

$$k_d \Delta x_2 > m_2 g. \tag{18}$$

It also indicates that the steady-state force to be generated by the hybrid magnet can be reduced by setting the upward force of the spring k_d appropriately.

According to the discussion in Section 2.2, the control current achieving the zero-power control is generally represented by

$$I(s) = -c_2(s)s(X_1(s) - X_2(s)), \tag{19}$$

where

$$c_2(s) = \frac{\tilde{h}(s)}{g(s)}. \tag{20}$$

3.2 Response to Direct Disturbance

It assumed for simplicity that the initial values of the variables are zero. From Eqs.(12) to (16) and (19), we get

$$X_1(s) = \frac{\tilde{k}_1(s)(t_2(s) + \tilde{k}_2(s))}{t_c(s)} X_0(s) + \frac{\tilde{k}_2(s)}{t_c(s)} F_d(s), \tag{21}$$

$$X_2(s) = \frac{\tilde{k}_1(s)\tilde{k}_2(s)}{t_c(s)} X_0(s) + \frac{t_1(s) + \tilde{k}_2(s)}{t_c(s)} F_d(s). \tag{22}$$

where

$$t_1(s) = m_1 s^2 + c_1 s + k_1, \tag{23}$$

$$t_2(s) = m_2 s^2 + c_d s + k_d, \tag{24}$$

$$\tilde{k}_1(s) = c_1 s + k_1, \tag{25}$$

$$\tilde{k}_2(s) = k_i c_2(s) s - k_s \tag{26}$$

$$t_c(s) = t_1(s)t_2(s) + \tilde{k}_2(s)(t_1(s) + t_2(s)). \tag{27}$$

To estimate the stiffness for direct disturbance, the direct disturbance f_d is assumed to be stepwise, that is,

$$F_d = \frac{F_0}{s} \qquad (F_0 : \text{const}). \tag{28}$$

When the vibration of the floor is neglected ($x_0 = 0$), the steady-state displacement of the table is obtained as

$$\frac{x_2(\infty)}{F_0} = \lim_{s\to 0} \frac{t_1(s) + \tilde{k}_2(s)}{t_c(s)} = \frac{k_1 - k_s}{(k_1 - k_s)k_d - k_s k_1}. \tag{29}$$

Therefore, if

$$k_1 = k_s, \tag{30}$$

then

$$\frac{x_2(\infty)}{F_0} = 0, \tag{31}$$

for any finite value of k_d. Equation (31) shows that the suspension system between the isolation table and the floor has infinite stiffness statically because there is no steady-state deflection even in the presence of stepwise disturbance acting on the table.

The steady-state displacement of the middle table and the variation of gap are obtained as

$$\frac{x_1(\infty)}{F_0} = \frac{-k_s}{-k_s k_1} = \frac{1}{k_1}, \tag{32}$$

$$\frac{x_1(\infty) - x_2(\infty)}{F_0} = \frac{-k_1}{-k_s k_1} = \frac{1}{k_s}. \tag{33}$$

Equations (32) and (33) show that when downward force acts on the isolation table ($F_0 < 0$), the middle table moves downward and the gap increases.

4. EXPERIMENT

4.1 Experimental Setup

Figure 8 shows a schematic diagram of a single-axis apparatus fabricated for experimental study (Kishita *et al.*, 2004). The isolation table is supported by four coil springs and a pair of plate springs, which operate as k_d in Fig.7. The middle table is also supported by four coil springs and a pair of plate springs, which operate as k_1 in Fig.7. The plate springs restrict the motion of the isolation table and the middle table to one translational motion in the vertical direction. An electromagnet is on the middle table, and permanent magnets are on the isolation table. The zero-power control is realized by this hybrid magnet to produce negative stiffness. An auxiliary electromagnet for adjusting the positive stiffness and adding damping is set on the base. Figure 9 shows a photograph of the experimental apparatus.

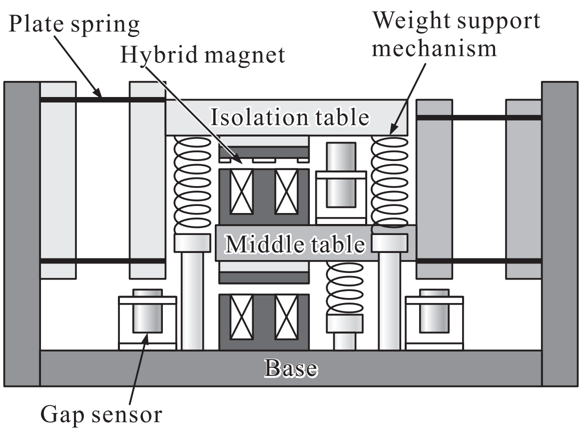

Fig.8 Schematic diagram of the experimental apparatus

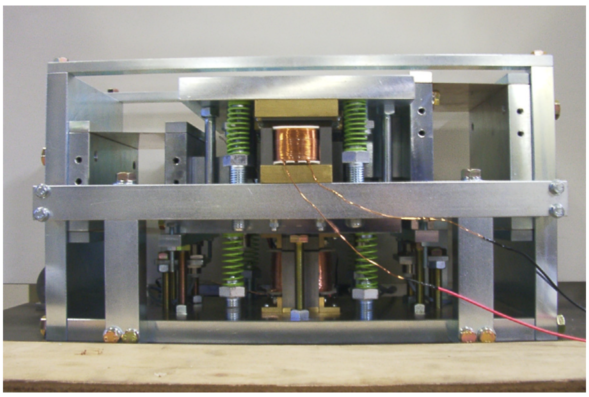

Fig.9 Photo of the apparatus

4.2 Experimental Results

First, zero–power control was realized when the middle table was fixed. Next the middle table was released. Then the springs for weight support mechanism and the auxiliary electromagnet were adjusted to satisfy Eq.(30).

Figure 10 presents the measurement results when weights are put on the isolation table to produce static direct disturbance. The displacements of the isolation table and the middle table are plotted to *downward* force produced by weights. When the force is in a range of 0 to 10 [N], the displacement of the isolation table is quite small so that high stiffness is achieved. When the force is over about 10 [N], the isolation table moves upward. The reason is explained as follows. When downward force acts on the isolation table, the gap between the isolation table and the electromagnet increases as mentioned in Section 3.2. When the gap increases, the gap-force coefficient of the magnet k_s decreases (Mizuno, 2002) so that the negative stiffness produced by zero-power control becomes lower. It indicates that the isolation table moves upward as observed in Fig.10.

The value of k_s can be adjusted by changing the initial compressed length of the springs for weight support. When the length is set to be larger, the steady force $\bar{f}_e$ increases so that k_s becomes larger. Figure 11 shows a force-displacement characteristic when the mass of the isolation table increases by 1.9kg and the above-mentioned adjustment for making k_s equal k_1 is carried out. Although a steady downward force caused by the increase of mass acts on the isolation table, the displacement of the isolation table is kept to be small.

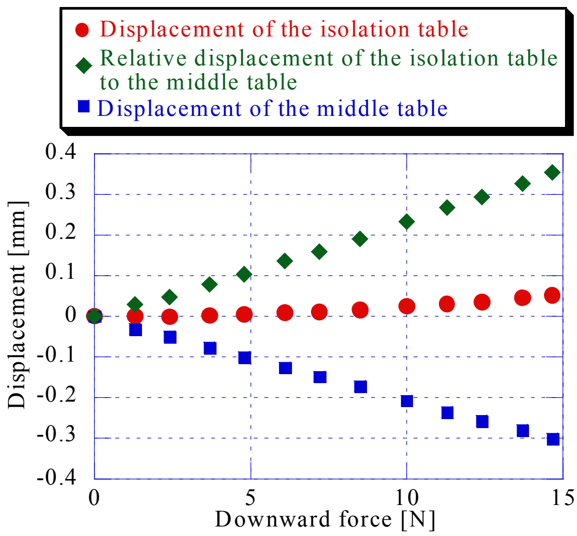

Fig.10 Response to static direct disturbance

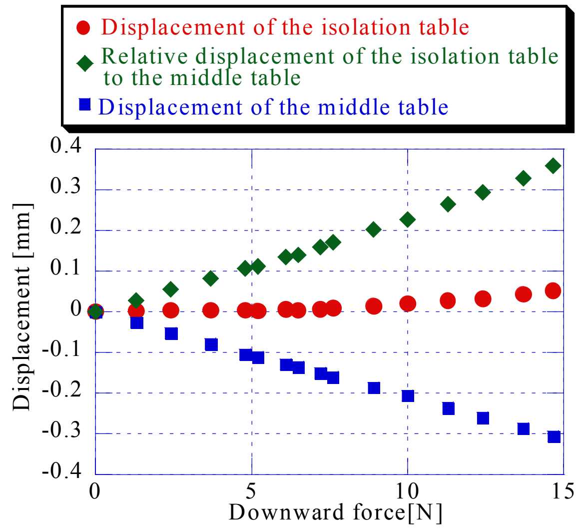

Fig.11 Response to static direct disturbance when a weight of 1.9kg is added to the isolation table.

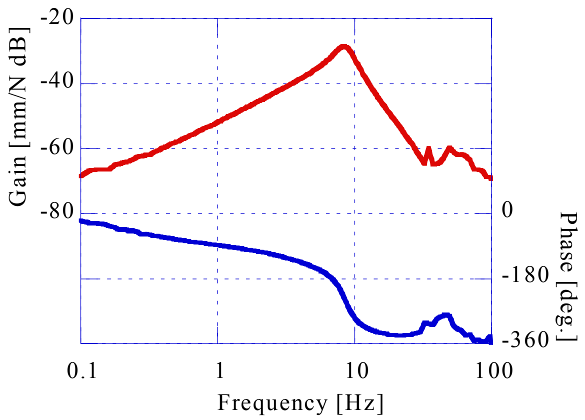

Fig.12 Frequency response of the isolation table to direct disturbance

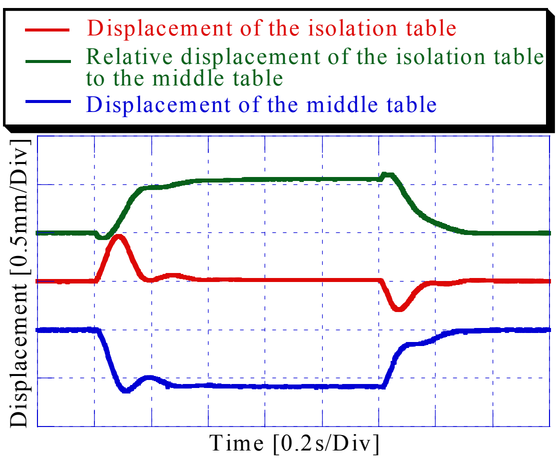

Fig.13 Step response to a stepwise direct disturbance

Figure 12 shows a frequency response of the isolation system. In measuring the frequency response, the auxiliary electromagnets are used to produce sinusoidal disturbance force to the isolation table, and the displacement of the isolation table was measured by the gap sensor. It is observed from this figure that high stiffness is achieved in a low frequency region. Figure 13 shows a response to stepwise direct disturbance whose amplitude is 10 [N]. It is observed that the transient response is damped well.

5. CONCLUSIONS

Vibration isolation system using zero-power magnetic suspension with a weight support mechanism was studied both theoretically and experimentally. It was pointed out that the structure of vibration isolation system becomes simpler than the original one. It was shown analytically that infinite stiffness is achieved by setting the amplitude of negative stiffness to equal that of positive stiffness independently of the weight suspension mechanism. The zero-power control was realized in the fabricated apparatus; the positive stiffness was adjusted to be equal to the negative stiffness. Consequently the high stiffness against direct disturbance was realized. The efficacy of the modified system was confirmed experimentally.

ACKNOWLEDGEMENT

This work is financially supported in part by a Grant-in-Aid for Scientific Research (B) from the Ministry of Education, Culture, Sports, Science and Technology of Japan, and a research grant from Suzuki Foundation.

REFERENCES

Kishita, D., Takasaki, M., Ishino, Y., Hoque, M.E. and Mizuno, T. (2004). Introduction of Weight Suspension Mechanism to Vibration Isolation System Using Zero-Power Magnetic Suspension, *Proc. 7th International Conference on Motion and Vibration Control*, 133.

Mizuno, T. (2002). Vibration Isolation System Using Zero-Power Magnetic Suspension, *Preprints of 15th World Congress IFAC*, 955.

Mizuno, T. and Takemori, Y. (2002). A Transfer-Function Approach to the Analysis and Design of Zero-Power Controllers for Magnetic Suspension System, *Electrical Engineering in Japan*, Vol.141, No.2, pp.67-75.

Mizuno, T. (2003). Vibration Isolation System Using Zero-Power Magnetic Suspension (5th report: Hybrid Suspension Mechanism), *Proc. Dynamics and Design Conference 2003*, 103 (*in Japanese*).

Yasuda, M. and M. Ikeda (1993). Double-Active Control of Microvibration Isolation Systems to Improve Performances (Application of Two-Degree-of-Freedom Control). *Transactions of the Japan Society of Mechanical Engineers*, C, **59**, 562, pp.1694-1701 (*in Japanese*).